

Impact of atmospheric anthropogenic nitrogen on new production in the northern Indian Ocean: Constrained based on satellite aerosol optical depth and particulate nitrogen levels

V.V.S.S. Sarma^{1,2}, B. Sridevi¹, Ashwini Kumar³, S. Bikkina³, V.R. Kumari¹, P. Bikkina³, K. Yadav¹ and V.D. Rao⁴

¹National Institute of Oceanography, Regional Centre,
176 Lawsons Bay Colony, Visakhapatnam, India

²Academy of Scientific and Innovative Research, Ghaziabad, India

³National Institute of Oceanography, Dona Paula, Goa, India

⁴National Centre for Coastal Research, Ministry of Earth Science,
Velacherry, Chennai, India.

Abstract

Aerosols are one of the significant external sources of soluble reactive nitrogen to the surface ocean and their deposition affects the phytoplankton's primary productivity and associated carbon sequestration. Owing to rapid industrialization over South and Southeast Asia, an increasing trend in atmospheric pollutants was observed over the northern Indian Ocean. To assess the contribution of the aeolian supply of inorganic nitrogen to the northern Indian Ocean (NIO), we have compiled the available data in marine aerosols collected over this basin between 2001 and 2020. Based on the observed relationship of mass load, particulate nitrate and ammonium concentrations over the NIO with the corresponding satellite-derived anthropogenic aerosol optical depth (AAOD) values, the temporal, spatial and long-term variabilities were derived over the NIO for the past two decades. In particular, high aerosol mass load, nitrate and ammonium levels were observed in the coastal aerosols of peninsular India during fall and winter and the least in summer. The basin-wide budget calculations revealed that atmospheric input of inorganic nitrogen to the Arabian Sea is higher (AS; 1.7 Tg/y) compared to the Bay of Bengal (BoB; 0.9 Tg/y) and accounts for ~30% of the total external sources of nitrogen to the NIO. The new production, supported by external sources of nitrogen, contributes to ~23 and 53% of export production to the oxygen minimum zone (OMZ) in the AS and BoB respectively. A significant rate of increase in the aerosol mass load ($0.05\text{--}1.67 \mu\text{g m}^{-3} \text{y}^{-1}$), nitrate ($0.003\text{--}0.04 \mu\text{g m}^{-3} \text{y}^{-1}$) and ammonium ($0.006\text{--}0.11 \mu\text{g m}^{-3} \text{y}^{-1}$) concentrations was observed between 2001 and 2020, likely because of the growing emission of anthropogenic pollutants over South and Southeast Asia and their subsequent long-range atmospheric transport to the NIO. Overall, these results suggest that enhanced contribution of atmospheric nitrogen may potentially increase 1) the N/P ratio of the surface ocean, which has an impact on the phytoplankton composition, 2) enhanced export production may intensify OMZ and 3) increase in sequestration of atmospheric CO₂. The decrease in primary production due to global warming is reported due to a decrease in vertical nutrient supply, however, the increase in atmospheric deposition of nutrients may compensate. Therefore, ocean models must couple with atmospheric models for a better forecast of oceanic response to climate change in the NIO.

Keywords: Aerosol optical depth, nutrients, dry deposition, primary production, northern Indian Ocean

1. Introduction

The aeolian transport, from the continent to the ocean, is recognized as one of the important pathways for nutrient supply to the surface ocean¹⁻⁴. An increase in phytoplankton biomass and primary production have been reported due to the deposition of atmospheric nutrients in the global ocean⁵⁻⁹. The impact is relatively more significant in the northern hemisphere compared to its southern counterpart mainly due to the larger landmass and more human activity in the former region^{10,11}. The global aeolian dissolved inorganic nitrogen (DIN) is reported to be almost equivalent to that of riverine sources^{7,12}. Therefore, the long-range transport of atmospheric DIN in the continental outflows to the marginal seas and downwind open ocean waters may have a significant impact on marine primary productivity.

The northern Indian Ocean is surrounded by land from three sides, where one-third of the world population is dwelling close to the coast. Several fast-growing cities are situated along the coast of the northern Indian Ocean resulting in a high contribution of anthropogenic aerosols to the atmosphere¹³⁻¹⁹. Hence, this region is classified as one of the hotspot regions in the global ocean with the highest rate of increase in anthropogenic aerosols^{20,21}. Seasonal reversal of wind pattern²² (Scott and McCreary, 2001) leads to variability in sources and composition of aerosols over the north Indian Ocean (NIO)^{14,23-25}. Nitrogen is reported as one of the severe limiting nutrients in the NIO (Valsaraj and Rao, 1994; Anju et al., 2020) resulting in the fixation of atmospheric nitrogen (eg: Kumar et al., 2017; Ahmed et al., 2017; Sarma et al., 2020; Kumari et al., 2022a). An increase in primary production and phytoplankton community change due to the deposition of atmospheric nutrients were reported in the Bay of Bengal (Yadav et al., 2016; Kumari et al., 2022b). Based on numerical models and remote sensing data, a significant increase in surface chlorophyll-a associated with atmospheric aerosol deposition has been reported from the NIO^{8,26-28}. In addition, efforts have been made to measure the chemical composition of aerosols under the aegis of several national and international programs in India^{14,19,23,25,29-34}. Combining several snapshot measurements, Srinivas and Sarin³¹ estimated that dry deposition of inorganic nutrients supports ~13% of the surface primary production in the Bay of Bengal (BoB) whereas ~5% in the Arabian Sea (AS) during the dry period. Similarly, Yadav et al.³² highlighted that ~70% of the total suspended particulate matter (TSP) was deposited within 10 km from the coast and can support 3 to 33% of the coastal surface primary production during fall and winter seasons in the BoB. In addition to primary production, the dry deposition of nitrogen can significantly enhance the N/P ratio in the surface waters which could eventually affect the phytoplankton composition³². Most of these estimations were carried out based on snapshot

measurements, however, the contribution of atmospheric nutrients to the basin-wide primary/new production is unknown.

Recent studies have found a decrease in the dissolved oxygen concentrations in the sub-surface layers in the BoB and an increase in primary/export production, due to the external supply of nutrients, may turn this region into a dead zone³⁵. The weakening of the vertical supply of nutrients and a decline in primary production was reported due to the rapid warming of the tropical Indian Ocean^{36,37}. On the other hand, the increasing rate of atmospheric pollutants over South and Southeast Asia was reported with a dominant increase in NO_x and SO_x from the middle of 2000³⁸. Such a rapid increase in NO_x may enhance particulate nitrogen deposition over the northern Indian Ocean leading to a possible increase in primary production in future. It is also possible that rapid warming associated with a weaker vertical supply of nutrients (upwelling) may be compensated by the deposition of nutrients from the atmosphere to sustain primary production. Sporadic studies on the chemical composition of aerosols revealed a significant fraction of aerosols over the northern Indian Ocean were contributed by anthropogenic sources^{14,19,23,25,31,32,34}. The increase in anthropogenic aerosol optical depth (AAOD) was reported in the BoB over the past two decades²¹. However, the trends in the concentrations of reactive nitrogen and their influence on surface primary production due to their subsequent deposition on the surface ocean are unknown. Therefore, the objective of the present study is to 1) quantify the spatial, temporal and long-term pattern of inorganic nitrogen concentrations in the marine boundary layer (MBL) of the northern Indian Ocean using the available measured data as well as satellite-derived AOD over the northern Indian Ocean, 2) quantify inorganic nitrogen inputs through atmospheric deposition and their contribution to new production and 3) evaluate the long-term trends in atmospheric deposition of inorganic nitrogen over the northern Indian Ocean.

2. Methodology and study area

2.1. Mass load, nitrate and ammonium concentrations in the marine aerosols over the NIO

The measured mass load, nitrate and ammonium concentrations of dry aerosols over the NIO between 2006 and 2020 data were used in this study during different seasons. The coverage was relatively good in the northeastern Indian Ocean (BoB) compared to the northwestern Indian Ocean (AS). The dates of the collection of samples and the region of the collection were given in Table 1. Ambient aerosol mass load over the NIO was assessed by the difference in filter weights before and after collection. The concentrations of nitrate and ammonium were measured using the Ion Chromatography techniques with suppressed conductivity detection. The details of the measurements and their precisions were given elsewhere^{14,23,25,32}.

2.2. Computation of anthropogenic aerosol optical depth (AAOD)

Since inorganic nitrogen (nitrate and ammonium) mainly enters the atmosphere through anthropogenic sources, the fraction of AOD contributed by the anthropogenic sources needs to be computed from the total AOD. We have obtained total AOD data at $1 \times 1^\circ$ grid resolution at 470 nm, 550 nm and 860 nm wavelengths from the Moderate Resolution Imaging Spectroradiometer Terra satellite (MODIS) collection 6.1 and level 3 from 2001 to 2019 (<https://ladsweb.modaps.eosdis.nasa.gov/search>). The Level 3 (L3) MODIS AOD atmosphere products data is a global-gridded science product. The fine mode fraction of AOD was computed from spectral AOD and fine-mode AOD (given as aerosol_optical_Depth_small-Ocean)³⁹. The error on the total AOD is $\pm 0.03 + 5\%$ of AOD⁴⁰. The fraction of anthropogenic AOD (AAOD) from total AOD was estimated following Kaufman et.al.⁴¹. The estimation of the anthropogenic component from MODIS total AOD uses several assumptions. They are a) the fine fraction of aerosol is constant to the AOD for a given aerosol type. Smoke and pollution are assumed to be mostly contributed to fine aerosols, whereas dust and marine components contribute to coarse aerosols. b) All smoke is considered to be of anthropogenic origin and all dust originated naturally. c) It is assumed that wildfires contribute $\sim 20\%$ of biomass burning and anthropogenic sources contribute up to 10% of the dust. d) MODIS-derived fine fraction is highly correlated with a true fine fraction with small errors. e) Based on AERONET and MODIS analysis^{41,42} the baseline marine aerosol optical thickness is assumed to be 0.06 ± 0.01 under calm conditions.

According to Kaufman et al.⁴¹ total aerosol optical thickness (τ_{550}) is defined as the sum of anthropogenic (τ_{anth}) from pollution and smoke + dust (τ_{dust}) + baseline marine (τ_{mar}) sources. The same can be written as

$$\tau_f = f_{550} \times \tau_{550} = f_{anth} \times \tau_{anth} + f_{dust} \times \tau_{dust} + f_{mar} \times \tau_{mar} \quad (1)$$

Here f_{mar} , f_{dust} , and f_{anth} are fraction fine particles from marine, dust and anthropogenic sources and they are derived from MODIS whereas τ_{mar} is determined from AERONET. The total fine fraction (f_{550}) and optical thickness (τ_{550}) were derived by MODIS. Based on this,

$$\tau_{anth} = [(f_{550} - f_{dust}) \tau_{550} - (f_{mar} - f_{dust}) \tau_{mar}] / (f_{anth} - f_{dust}) \quad (2)$$

The complete details of the estimations and constants used are given in Kaufman et al.⁴¹. In the present study, we used MODIS collection 6.1 AOD data whereas Kaufman et al.⁴¹ used collection 4 data to derive the constants, therefore, we calculated the constants f_{mar} , f_{dust} , and f_{anth} using MODIS collection 6.1 data for the same regions and periods that of Kaufman et al.⁴¹. We obtained f_{mar} , f_{dust} , and f_{anth} as

0.32, 0.48, and 0.77 respectively and the computation of the fraction of anthropogenic aerosols carries an uncertainty of up to $\pm 30\%$.

The weighted linear regression analysis was conducted on the monthly mean data of anthropogenic AOD, aerosol nitrate and ammonium concentrations in the selected regions in the northwest AS (Nwas), northeast AS (NEAS), southwest AS (SWAS), southeast AS (SEAS), northern BoB (NBoB), southeast BoB (SEBoB) and southwest BoB (SWBoB; Figure 1) regions between 2001 and 2020 to obtain long-term trends. The NEAS and NBoB boxes represent the regions that receive high anthropogenic aerosols from Indo-Gangetic Plain (IGP) region, whereas the SEAS region receives from mainland India. Both Nwas, SWAS in the AS and SWBoB, SEBoB boxes in the BoB are away from the anthropogenic aerosol source regions.

2.3. Dry depositional flux of nitrate and ammonium

The dry depositional fluxes of NO_3^- and NH_4^+ were computed following:

$$\text{Dry-Deposition flux} = C_{\text{measured}} * V_{\text{dry}} \quad (3)$$

Where C_{measured} is the concentration of nitrate or ammonia in the aerosols and V_{dry} is the dry deposition velocity, which is estimated to be 1.0 and 0.1 cm sec^{-1} , respectively for nitrate and ammonia in the PM_{10} . The low V_{dry} for NH_4^+ (0.1 cm sec^{-1}) is considered due to its predominant occurrence in the fine mode^{23,43,44}. The uncertainty associated with the computation of dry deposition fluxes can be by a factor of 3 due to several factors including wind speed, terrain roughness, particle composition etc³¹.

2.4. Computation of long-term trends in the selected region

To understand the long-term changes of all these parameters on a seasonal scale, data are prepared into seasonal means (winter-December, January, February; Spring – March, April and May; Summer – June, July, August and September and Fall – October and November) and then liner trend analysis was performed on all the parameters.

We have determined the trends and statistical significance of the parameters studied following Santer et al⁴⁵. The trends of the parameters were computed using a least-square fit method for each seasonal data as:

$$x(t) = a + bt, \text{ for } t = 1, \dots, nt$$

The significance of the computed trends was evaluated following Santer et al.⁴⁵, in which regression residuals ($e(t)$) are defined as:

$$e(t) = x(t) - x_m(t); \text{ for } t = 1, \dots, nt$$

x_m is the mean value and for statistically independent values of $e(t)$, the standard error of the slope, b , is defined as:

$$S_b = Se / (\sum(t-t_m)^2)^{0.5}$$

where t_m is the mean and Se^2 is the variance of the residuals about the regression line, is given by

$$Se^2 = (1/n_r - 2) * \sum e(t)^2$$

Whether the $e(t)$ trend is significantly different from zero is tested by computing the ratio between the estimated trend and its standard error

$$t_b = b / s_b$$

We noticed that $e(t)$ is not statistically dependent hence autocorrelation method involving sample size is used following Santer et al⁴⁵. The seasonal trend analysis results and their significance between 2001 and 2020 are given in Table 2.

3. Results

3.1. Importance and meteorological condition of the Northern Indian Ocean (NIO)

The NIO is surrounded by the deserts in the Oman, Somalia, Iran and Thar regions in the west (Arabian Sea), and surrounded by highly populated underdeveloped nations such as Bangladesh, Burma, Thailand etc., in the eastern basin (Bay of Bengal). The NIO is influenced by the seasonally reversing monsoonal winds that blow from the northeast direction during winter (November to February, called northeast monsoon) and southwest direction during summer (June to September; called southwest monsoon; Wiggert et al., 2005). The air mass over the NIO is strongly influenced by the continental pollution sources (eg: biomass burning and fossil-fuel combustion) in winter (Bikkina et al., 2011; 2021; Kumar et al., 2012; Ashwini et al., 2020). The Arabian Sea receives mineral dust particles in summer from the desert region (Tindale and Pease, 1999; Prospero et al., 2002). In the case of the Bay of Bengal, the continental pollution from the Indian subcontinent is received during summer and Southeast Asia during winter (Kumari et al., 2022). More than 80% of the annual precipitation occurs during summer and scarce or episodic rainfall occurs during winter (Soman and Kumar, 1990).

3.2. Distribution of anthropogenic aerosols (AAOD) over the northern Indian Ocean

The climatological mean AAOD (2001-2020) displayed significant spatial and temporal variations over the northern Indian Ocean, which may be partially attributed to meteorological factors such as the seasonal reversing of wind patterns. The levels of AAOD were relatively higher along the Indian coast and rapidly decreased towards the open oceanic region (Fig. 1). The levels of AAOD increased

rapidly from September to April and lower levels were noticed between May and August (Fig. 1). The high levels of AAOD were observed along the east coast of India between November and March with the peak in December and January. In contrast, high levels of AAOD were observed from October to March with a peak in October to November along the west coast of India. A clear north-south gradient in AAOD levels was observed in the BoB with relatively higher values in the north and a decreasing trend towards the south. Such decreasing pattern was absent in AAOD and was almost missing in the AS.

3.3. *Distribution of measured mass load, nitrate and ammonium concentrations in aerosols over the northern Indian Ocean*

The distribution of measured climatological mass load, nitrate and ammonium concentrations in the aerosols were presented in Figure 2a. The mass load was higher along the Indian coast and northern BoB compared to the offshore and southern BoB. Higher concentrations of nitrate and ammonium were observed along the Indian coast than offshore (Fig. 2b,c). AAOD values displayed a significant linear relationship with the mass load, nitrate and ammonium concentrations in the AS and BoB (Fig. 3). The slope of the relationship was different in the two basins. For instance, the slope of the relationship of AAOD with mass load, nitrate and ammonium was almost double in the BoB (115.8, 3.4, and 7.6 respectively) than in the AS (54.8, 1.7 and 3.3 respectively). The relationship yielded the following regression equations:

$$\text{Mass} = 115.84 * \text{AAOD} + 11.322; r^2=0.54 (p<0.001) \quad (\text{BoB}) \quad \text{---} \quad (4)$$

$$\text{NO}_3^- = 3.42 * \text{AAOD} + 0.004; r^2=0.51 (p<0.001) \quad (\text{BoB}) \quad \text{---} \quad (5)$$

$$\text{NH}_4^+ = 7.65 * \text{AAOD} - 0.59; r^2=0.58 (p<0.001) \quad (\text{BoB}) \quad \text{---} \quad (6)$$

$$\text{Mass}=54.85 * \text{AAOD} + 21.47; r^2=0.62 (p<0.001) \quad (\text{AS}) \quad \text{---} \quad (7)$$

$$\text{NO}_3^- = 1.71 * \text{AAOD} + 0.31; r^2=0.69 (p<0.001) \quad (\text{AS}) \quad \text{---} \quad (8)$$

$$\text{NH}_4^+ = 3.29 * \text{AAOD} + 0.32; r^2=0.68 (p<0.001) \quad (\text{AS}) \quad \text{---} \quad (9)$$

3.4. *Temporal and spatial variations in the mass load, nitrate and ammonium concentrations in the aerosol over the northern Indian Ocean*

The monthly variations in climatology (2001-2020) of the computed mass load, nitrate and ammonium concentration varied from 0.5 to 100, 0 to 2 and 0 to 3.5 $\mu\text{g m}^{-3}$ respectively in the NIO. Higher concentrations of mass, nitrate and ammonium concentrations were observed in the BoB than in the AS. The high concentrations of mass ($>50 \mu\text{g m}^{-3}$), nitrate ($>1.5 \mu\text{g m}^{-3}$) and ammonium ($>2.5 \mu\text{g m}^{-3}$) were observed along the coastal BoB with high concentrations between October and April than in

other seasons (Fig. 4-6). On the other hand, high concentrations of nitrate and ammonium were observed in the south-eastern AS from October to April compared to other months (Fig. 5 and 6). A perennial low concentration of nitrate ($<0.5 \mu\text{g m}^{-3}$) and under detection limits of ammonium was observed in the southern BoB. Relatively high concentrations of nitrate and ammonium were observed in the offshore regions in the AS from October to January while it was from January to April in the case of the BoB.

3.5. Dry depositional flux of nitrate and ammonium in the northern Indian Ocean

The dry depositional flux of nitrate and ammonium varied between 0-1.8 and 0-0.3 $\text{mgN m}^{-2} \text{d}^{-1}$ in the northern Indian Ocean respectively (Fig. 7-8). Both nitrate and ammonium fluxes were higher in the north-western BoB (>1.4 and $>0.25 \text{mgN m}^{-2} \text{d}^{-1}$ respectively) followed by south-eastern AS from October to April (0.6-1.0 and 0.1-0.15 $\text{mgN m}^{-2} \text{d}^{-1}$ respectively). Assuming the C/N ratios of 6.6, and deposited nitrate and ammonium were completely utilized by the phytoplankton, the contribution of atmospheric deposition of inorganic nitrogen to the primary production in the surface ocean was 0-18.5 $\text{mgC m}^{-2} \text{d}^{-1}$ in the northern Indian Ocean (Fig. 9).

3.6. Long-term trends in AAOD, mass, nitrate and ammonium fluxes in the northern Indian Ocean

The seasonal long-term trends in AAOD, mass, nitrate and ammonium fluxes were derived in the selected regions (Fig. 1) in the northern Indian Ocean. The rate of AAOD was significant in all the regions at a 99% confidence interval, except in the SWBoB and SEBoB where it is either low or insignificant (Table 2). The rate of increase in AAOD varied between 0.002 and 0.014/y with lower rates in the SWAS (0.003-0.005/y) and higher in the NEAS, SEAS and NBoB (0.007-0.014/y). The lowest rate of increase with low significance ($p < 0.05$) was observed in the SWBoB (0.002-0.003/y). Within the seasons, a high rate of increase in AAOD was noticed during the fall monsoon and either decreasing or insignificant trends were observed during summer.

The rate of increase in mass load varied between 0.11 and 1.67 $\mu\text{g m}^{-3} \text{y}^{-1}$ in the northern Indian Ocean. The highest rate of the mass load was observed in the NBoB (0.59 to 1.67 $\mu\text{g m}^{-3} \text{y}^{-1}$) during all seasons, except summer, followed by SEAS (0.66-0.80 $\mu\text{g m}^{-3} \text{y}^{-1}$) and NEAS (0.12 to 0.66 $\mu\text{g m}^{-3} \text{y}^{-1}$) and the least rate of increase was noticed in the SWAS (0.14-0.26 $\mu\text{g m}^{-3} \text{y}^{-1}$) and SEBoB (-0.04 to 0.25 $\mu\text{g m}^{-3} \text{y}^{-1}$). Except in the NBoB and SEAS, the rate of mass load decreased during summer (Table 2).

The rate of increase in nitrate and ammonium in the aerosols ranged between 0.003 to 0.049 $\mu\text{g m}^{-3} \text{y}^{-1}$ and 0.01 to 0.11 $\mu\text{g m}^{-3} \text{y}^{-1}$ respectively in the northern Indian Ocean. The rate of increase in nitrate was higher in the SEAS and NBoB (0.02 to 0.05 $\mu\text{g m}^{-3} \text{y}^{-1}$) during all seasons, except summer. Except

in NBoB and SEAS, negative (decrease) trends in nitrate were noticed during summer. A higher rate of increase in ammonium was observed in the NBoB and SEAS (0.04 to $0.11 \mu\text{g m}^{-3} \text{y}^{-1}$) than in other regions (Table 2).

4. Discussion

4.1. *Spatial variations in atmospheric deposition of nitrogen and its contribution to surface primary production in the northern Indian Ocean*

The northern Indian Ocean receives anthropogenic rich aerosols during winter associated with northeasterly winds while the dominance of mineral dust and sea salt is observed during summer months when prevailing winds are southwesterly^{14,16,46-48}. The primary source of dust to the northern Indian Ocean comes from the Nubian desert, the Arabian Peninsula, Iran, Pakistan, Afghanistan and North-West India with maximum activity between May and October⁴⁹⁻⁵². The fraction of AAOD to the total AOD was higher during winter and spring (November-April; 60-70%) than in summer (30-40%) over the northern Indian Ocean due to the influx of anthropogenic rich aerosols derived from the surrounding continents where >30% of the global population dwells^{21,53}. The perennial high levels of AAOD were observed along the Indian coast with the rate of increase being the highest over the globe^{20,21} and it was attributed to a significant increase in the contribution of anthropogenic emissions from the Indo-Gangetic Plain (IGP) and southeast Asia.

The climatological mean (2001-2020) derived mass load, nitrate and ammonium concentration were high along the Indian coasts from October to April due to prevailing terrestrial winds resulting in the input of anthropogenic aerosols. The sharp gradient in aerosol mass, nitrate and ammonium concentration was observed from the coast towards the open oceanic region mainly due to the proximity of the emission source region. During a similar period, the western BoB receives aerosols from the biomass burning from the Indo-Gangetic Plain (IGP) region and southeast Asia due to dominant winds from the northeast direction resulting in enhanced mass load, nitrate and ammonium concentration along with the coastal and northern BoB^{54,55}. These are the least during summer due to washout from the atmosphere via heavy monsoonal precipitation⁵⁶.

The AAOD displayed a linear relationship with nitrate and ammonium concentrations in the aerosols at 99% significance levels (See equations 4-9) suggesting that anthropogenic sources are dominant contributors of dissolved inorganic nitrogen to the aerosols over the northern Indian Ocean. Perennial high concentrations of nitrate and ammonium were observed along the Indian coast (Fig. 5,6); particularly high levels from October to April months. The dry depositional flux of nitrate and ammonium varied from $0-1.8$ and $0-0.3 \text{ mgN m}^{-2} \text{ d}^{-1}$ in the northern Indian Ocean with higher fluxes

along the Indian coastal region and northern BoB due to proximity to the source emissions (Fig. 7,8). The deposition of atmospheric nitrogen may enhance primary production in the surface ocean^{1,31}. Recently Kumari et al. (2022) measured an increase in primary production by 3-19% due to the deposition of atmospheric aerosols in the coastal Bay of Bengal whereas Yadav et al. (2016) noticed increase by 3 to 33%. Episodic increase in phytoplankton blooms associated with dust storms was reported in the northern Indian Ocean and attributed to the deposition of atmospheric nutrients^{8,26-28,51}. Severe nitrogen limitation to primary production was reported in the northern Indian Ocean (Anju et al., 2020; Sarma et al., 2013; Valsaraj and Rao, 1994). Assuming that the deposited inorganic nitrogen (nitrate and ammonium) on the surface ocean is completely utilized by the phytoplankton, it may support the primary production of 0-18.5 mgC m⁻² d⁻¹ in the northern Indian Ocean (Fig. 9b, c).

To examine the contribution of primary production supported by atmospheric deposition of inorganic nitrogen to total primary production, the surface primary production data was measured using the radio-active carbon (¹⁴C) tracer incubation method for comparison. The seasonal and spatial variability in primary production in the northern Indian Ocean was measured between 1994 and 2019 during various national and international programs⁵⁷⁻⁶³. The upper 5 m integrated primary production varied between 7.8 and 387 mgC m⁻² d⁻¹ in the AS and 6.8 to 225 in the BoB (Fig. 9a). Assuming the entire dry deposition of inorganic nitrogen is utilized by the phytoplankton, the air-to-sea flux of nitrogen is converted to equivalent carbon produced by the phytoplankton primary production using a canonical Redfield ratio (C/N ratio of 6.6). The primary production supported by atmospheric borne nitrate and ammonium between 2001 and 2020 was used to evaluate its contribution to the total primary production in the upper 5 m depth. In the case of primary production measurements made before the year 2000, the primary production derived from the climatological mean nitrate and ammonium deposition rates was considered for comparison due to the lack of AOD data. The contribution of primary production, supported by atmospheric deposition of nitrogen, to total primary production in the upper 5 m of the water column ranged between 1.1 and 45% (mean of 14±7%) in the BoB whereas it was 1 to 54 (11±8%) in the AS (Fig. 9d). Based on the depositional flux estimated using measured dissolved inorganic nitrogen, the contribution of atmospheric nitrogen to surface primary production was reported to vary between 3 and 33% during different seasons with a maximum during winter in the coastal BoB^{23,32}. Srinivas et al.²³ estimated that <13% of the primary production in the entire BoB is supported by atmospheric deposition of nitrogen whereas it is <5% in the AS^{31,64}. The present estimations suggested that atmospheric deposition of nitrogen contributed almost equally to the surface primary production in the AS and BoB than hitherto estimated that higher contribution in the latter than the former basin^{23,31} (Fig. 9d).

4.2. Contribution of external sources of nitrogen to the northern Indian Ocean

The northern Indian Ocean is a highly productive region within the Indian Ocean with relatively higher production in the AS than BoB due to various oceanic processes which include the occurrence of strong upwelling and convective mixing during summer and winter respectively^{58,59,63}. In contrast, the absence of such strong mixing in the BoB due to strong salinity stratification results in low primary production^{59,65}. Due to the proximity to the land, the northern Indian Ocean receives a significant amount of nutrients through land-ocean (rivers and groundwater) and ocean-atmosphere (atmospheric deposition) boundaries. Due to stratification during non-monsoon periods with low inorganic nitrogen inputs to the surface, nitrogen fixation occurs and contributes significantly to the primary production in the northern Indian Ocean. Based on the available data in the recent literature and present depositional flux of nutrients from the atmosphere estimates, the contribution of external sources of nitrogen to the northern Indian Ocean was computed.

Several rivers, such as Ganges, Brahmaputra, Irrawady-Salween system, Godavari, Krishna, Mahanadi etc, opened to the BoB, whereas Narmada, Tapti, Mandovi-Zuari etc rivers are opened to the AS⁶⁶. The river discharge to the BoB is 3 times higher than that of the AS due to the discharge of more rivers in the former basin⁶⁷. Krishna et al.⁶⁶ estimated riverine inorganic nitrogen inputs to the AS and BoB to be 0.10 ± 0.03 and 1.74 ± 0.43 TgN/y and contribute to 0.7 ± 0.2 and 11.5 ± 3 TgC/y of new production respectively based on C/N ratio of 6.6 (Table 3).

The northern Indian Ocean has a very long coastline and the exchange of nutrients through submarine groundwater discharge (SGD) is a possible source of nutrients. The higher concentrations of nutrients, by an order of magnitude, in the groundwater than in coastal waters were reported⁵¹. The estimated SGD flux of dissolved inorganic nitrogen was estimated to be 0.06 ± 0.03 and 0.102 ± 0.02 TgN/y to the AS and BoB, which supports 0.4 ± 0.2 and 0.7 ± 0.1 TgC/y of new production respectively.

The estimated long-term mean (2001-2020) flux of atmospheric nitrate and ammonium varied between 0-1.8 and 0-0.3 mg N m⁻² d⁻¹ in the northern Indian Ocean respectively with higher rates in the western BoB and eastern AS. The estimated deposition of atmospheric inorganic nitrogen over the entire AS and BoB is estimated to be 1.7 ± 0.4 and 0.9 ± 0.2 TgN/y respectively and it would support 11.2 and ~6.0 TgN/y of new production respectively in the AS and BoB.

The occurrence of nitrogen fixation was reported both in the AS and BoB during the inter-monsoon period. In the case of the AS, most of the measurements were taken in the eastern basin and few measurements were carried out in the western basin. Nitrogen fixation rates varied between 124 and 1500 $\mu\text{mol N m}^{-2} \text{d}^{-1}$ in the AS⁶⁸⁻⁷² with a mean of 532 ± 547 $\mu\text{mol m}^{-2} \text{d}^{-1}$, excluding the one outlier of

36000 $\mu\text{mol N m}^{-2} \text{d}^{-1}$, and extrapolating to the entire basin during spring inter-monsoon amounts to 4.4 TgN y^{-1} in the AS. The N_2 fixation rates in the BoB varied between 0.7 and 75.2 $\mu\text{mol m}^{-2} \text{d}^{-1}$ ⁷³⁻⁷⁵ with a mean of $10.5 \pm 12 \mu\text{mol m}^{-2} \text{d}^{-1}$ and extrapolating to the entire BoB amounts to $0.2 \pm 0.1 \text{ TgN y}^{-1}$. The equivalent to new production is estimated based on a C/N ratio of 6.6. Based on the synthesis of measured N_2 fixation data, the contribution of new production due to N_2 fixation is estimated as 29.0 and 1.3 TgC/y in the AS and BoB respectively. The low N_2 fixation in the BoB is attributed to the removal of phosphate in association with suspended particulate matter⁷⁶.

The total external sources of inorganic nitrogen to the AS and BoB come to 6.3 ± 4 and $2.0 \pm 0.4 \text{ TgN/y}$ respectively. The contribution of nitrogen fixation dominates (70%) followed by atmospheric deposition (27%) in the AS whereas river discharge (60%) followed by atmospheric deposition (30%) contributed to total external sources in the BoB. The contribution of SGD is minimal (1-3%) in both AS and BoB (Table 3). The external sources support 41.3 ± 26 and $19.5 \pm 3 \text{ TgC}$ of new (primary) production in the AS and BoB respectively.

Since most of the new production is exported to the twilight zone⁷⁷ (Dugdale and Goering, 1967), the contribution of new production by external sources to the export production is compared. The export production at 100 m was measured in the northern Indian Ocean from 1994 to 1996 and 2013 to 2015⁷⁸⁻⁸⁰. Seasonal variability in export production was measured in the AS whereas only measurements were conducted during the non-monsoon season in the BoB, therefore, some seasonal bias is anticipated in the latter basin. Based on these estimates, the export flux to the twilight zone was accounted to be 182 and 36 TgC/y in the AS and BoB respectively⁷⁸⁻⁸⁰. The total external sources of nitrogen supported new production contributed to 23 and 53% of the export production in the AS and BoB respectively and the remaining export production is contributed by nutrient upwelled from the subsurface water, either wind-driven coastal upwelling (Morrison et al., 1998) or eddy-driven upwelling (Sarma et al., 2018) and regenerated nutrients through microbial processes. Among the external sources, nitrogen fixation (16%) and atmospheric deposition (6%) contributed significantly to the export production in the AS whereas river discharge (31%) and atmospheric deposition (17%) contributed to the BoB. Therefore, the contribution of atmospheric deposition is significant not only to surface production but also to export production to the twilight zone in the northern Indian Ocean.

In this study, we have estimated the contribution of inorganic nitrogen to the surface ocean through dry depositional flux. Jickells et al. (2017) reported that organic nitrogen contributes about 1/3 of the total nitrogen deposition. A dominant fraction of organic nitrogen (40-50%) to the total nitrogen was reported in the Arabian Sea (Bikkina et al., 2021) and the Bay of Bengal (Bikkina et al., 2011).

Recently Rao et al. (2021) reported that dissolved organic nitrogen contributes to ~50% of the primary production in the Bay of Bengal in the absence of inorganic nitrogen. Due to the lack of spatial data on dissolved organic nitrogen in the aerosols, we could not account for their contribution to the total primary production in this study. On the other hand, the NIO is highly influenced by monsoonal precipitation and the contribution of wet deposition of nitrogen may be a highly significant nitrogen source to the surface ocean. Baker et al. (2021) reported that the acidity of the aerosols changes the lifetime of nitrate in the atmosphere and increases the ammonium resulting in the long-range transport of ammonium and deposition close to the coast in the case of nitrate under acidic conditions. The acidic nature of the aerosols over the Bay of Bengal was reported recently (Kumari et al., 2022) and its impact on partitioning of nitrate and ammonium is unclear. Nevertheless, the role of organic nitrogen and wet deposition to total nitrogen deposition and its contribution to the external sources and surface primary production needs further studies.

Bristow et al.³⁵ found that dissolved oxygen in the subsurface layers is at the tipping point with reference to oxygen levels in the oxygen minimum zone (OMZ) and an increase in external sources of nutrients may enhance primary and export productions that may further intensify oxygen levels leading to the formation of dead zones. In this context, our study highlights the contribution of atmospheric sources is significant, especially in the BoB (17%) than in the Arabian Sea (6%), which may intensify OMZ formation. Kurokawa and Ohara³⁸ found a rapid rate of increase in NO_x and SO_x in the atmosphere over South and Southeast Asia since the middle of 2000. This may enhance nitrogen deposition over the northern Indian Ocean which may increase primary and export production. These results underscore the need to examine the long-term trends of atmospheric nutrient concentrations in synchronous with the dissolved oxygen levels in the subsurface waters of both basins.

4.3. Long-term trends in atmospheric deposition of dust, nitrogen and its impact on primary production

The long-term trends in the AAOD, mass load, nitrate and ammonium concentrations in the selected regions were shown in Table 2. The rate of increase in AAOD was more than double in the eastern basin (NEAS and SEAS) ($0.007\pm 0.002/\text{y}$) than western basin (SWAS and NWAS) ($0.004\pm 0.001/\text{y}$) due to proximity to the source region of the Indian subcontinent in the former regions, except summer. The rate of increase in AAOD in the northern BoB was the highest ($0.01/\text{y}$) and it was insignificant in the southern BoB. The rate of increase in AAOD in the BoB was higher than earlier reports between 2000 and 2009 ($0.0077\pm 0.0003/\text{y}$) but lower in the case of the Arabian Sea ($0.006\pm 0.0002/\text{y}$)^{20,21} observed that the rate of increase in AAOD was significant between 2001 and 2019 in the northwestern and western coastal BoB but insignificant in the other regions (Yadav et al., 2021).

The computed mass load, nitrate, and ammonium concentrations in the aerosols displayed an increasing trend in the SWAS during all seasons but displayed negative trends in summer. A relatively higher rate of increase in mass load was observed in the eastern basin (NEAS and SEAS) than in the western basin (SWAS and NWAS) due to proximity to the source region from the Indian subcontinent. Within the seasons, a higher rate of increase in mass load was observed during fall monsoon in the NEAS, SWAS and NWAS whereas winter and spring in SEAS than in other seasons (Table 2). The annual mean rate of increase in mass concentration was also higher in the NEAS ($0.221 \pm 0.182 \mu\text{g m}^{-3} \text{y}^{-1}$), SEAS ($0.443 \mu\text{g m}^{-3} \text{y}^{-1}$) than in SWAS ($0.103 \pm \dots \mu\text{g m}^{-3} \text{y}^{-1}$) and NWAS ($0.109 \pm \dots \mu\text{g m}^{-3} \text{y}^{-1}$) suggesting that the eastern basin is receiving a significant amount of anthropogenic aerosols since past two decades than a western basin of AS. The highest increase in mass load was observed in the NBoB ($1.18 \mu\text{g m}^{-3} \text{y}^{-1}$) due to the receipt of major sources from the IGP and Southeast Asia²¹. The rate of increase in mass load was the least in the SEBoB ($0.05 \mu\text{g m}^{-3} \text{y}^{-1}$) and SWBoB ($0.34 \mu\text{g m}^{-3} \text{y}^{-1}$) due to being far from the source region. This study suggests that a significant increase in the mass of aerosols was noticed in the eastern AS and northern BoB in the northern Indian Ocean which may decrease the rate of increase in SST. Dong et al.⁸¹ observed that the rate of warming decreased in the northern Indian Ocean due to AAOD in the atmosphere. This impact was found to be stronger over the BoB than the AS due to higher levels of AAOD over the former than in the latter basin. Sarma et al.⁸² also reported a decrease in the rate of warming in the north-western BoB due to an increase in atmospheric pollutants between 1991 and 2011. However, the role of AAOD on SST needs further evaluation in the northern Indian Ocean.

Significant increasing annual mean trends in nitrate and ammonium concentrations were observed in the eastern (0.007 - 0.013 and 0.012 - $0.023 \mu\text{g m}^{-3} \text{y}^{-1}$ respectively) than western AS (0.002 - 0.003 and 0.004 - $0.005 \mu\text{g m}^{-3} \text{y}^{-1}$ respectively; Table 2) suggesting that the former region of the basin receiving higher nutrients through dry deposition. The increasing annual mean trends in nitrate and ammonium were higher in NBoB (0.034 and $0.076 \mu\text{g m}^{-3} \text{y}^{-1}$ respectively) than in SEBoB and SWBoB (0.001 - 0.01 and 0.005 - $0.013 \mu\text{g m}^{-3} \text{y}^{-1}$ respectively). The depositional rate of inorganic nitrogen concentrations increase by 135% in the NBoB followed by SWBoB (34%) and the least in the SEBoB (13%) between 2001 and 2020. In the case of AS, the increase in inorganic nitrogen was more in the NEAS (30%) and SEAS (44%) compared to NWAS (14%) and SWAS (11%). The mean rate of increase in primary production between 2001 and 2020 due to deposition of atmospheric inorganic nitrogen was higher in the NBoB ($2.5 \text{gC m}^{-2} \text{y}^{-1}$) followed by eastern AS (1.2 - $1.8 \text{gC m}^{-2} \text{y}^{-1}$), western AS (1.0 - $1.2 \text{gC m}^{-2} \text{y}^{-1}$) and southern BoB (0.6 - $0.8 \text{gC m}^{-2} \text{y}^{-1}$). Bindoff et al.⁸³ found that a decline in primary production is projected by $50 \text{gC m}^{-2} \text{y}^{-1}$ in the western AS whereas $30 \text{gC m}^{-2} \text{y}^{-1}$ in the eastern

AS and southern BoB, in contrast, an increase by $20 \text{ gC m}^{-2} \text{ y}^{-1}$ was reported in the NBoB and SEBoB between 2081-2100 relative to 1950-1900 under RCP 8.5 scenario. The decline in primary production by end of this century was attributed to the warming of the ocean, an increase in stratification and a weakening of nutrient supply through vertical mixing. In contrast, our study suggests that enhanced atmospheric pollution in future may compensate for nutrient decrease due to warming and stratification that may decrease the projected declining rates. Since the rapid increase in atmospheric pollution is already reported in South and South Asia³⁸ over the past two decades, atmospheric nutrient contribution may be significant in future and needs further evaluation.

Summary and Conclusion

The dry deposition of atmospheric nitrogen is hypothesized to be an important source of nutrients to the northern Indian Ocean. To quantify this, temporal and spatial variations in concentrations and depositional rates of inorganic nitrogen in the atmosphere were computed based on the relationship between measured nitrogen in the aerosols and satellite-derived anthropogenic aerosol optical depth (AAOD). The perennial high concentrations of mass load, nitrate and ammonium were observed in the aerosols over the eastern AS and western BoB with characteristic seasonality. A significant decrease in AAOD levels and concentrations of nitrogen was observed in the open oceanic region. This suggests that the Indian subcontinent could be one of the potential sources of pollutants, along with emissions from Southeast Asia, to the northern Indian Ocean. Relatively higher concentrations of nitrate and ammonium were observed in the aerosols during fall and winter and the least during summer due to heavy precipitation. The contribution of atmospheric deposition of inorganic nitrogen amounted to 1.7 and 0.9 TgN y^{-1} to the AS and BoB respectively. It accounts for ~30% of the external sources (river discharge, N_2 fixation and submarine groundwater discharge) of inorganic nitrogen to the northern Indian Ocean. The total external sources contribute 23 and 53% of the export production to the oxygen minimum zone (OMZ) in the AS and BoB respectively. The long-term variability in the mass load, nitrate and ammonium concentrations in the aerosols between 2001 and 2020 suggests a significant rate of increase due to a perennial increase in atmospheric pollution. This may result in a significant increase in primary and export production to OMZ and a decrease in the warming rate due to the blanketing effect.

The northern Indian Ocean harbours one of the most intense OMZs in the world and the oxygen levels in the OMZ are controlled by primary/export production and circulation of the intermediate waters. The nanomolar levels of oxygen are observed in the OMZ in the northern BoB and reported to be at the tipping point³⁵. This study suggests that atmospheric deposition is contributing to 30% of external nitrogen input to the northern Indian Ocean with a perennial increase in its contribution, therefore, the

organic matter flux to the OMZ may increase in future. This may lead to further intensification of the OMZ in the northern Indian Ocean. The atmospheric deposition not only increases inorganic nitrogen concentration but also the N/P stoichiometric ratio which may have a significant impact on the phytoplankton composition and therefore food web dynamics in the northern Indian Ocean³². While this study synthesizes a snapshot picture of aerosol composition in different seasons, however, to get a robust trend in nutrient supply and assess their impact on surface water processes, the time-series observations of atmospheric aerosol composition and associated nutrients over the northern Indian Ocean are essential, which enable us to understand the role of the human impact on ecosystem structure. Nevertheless, this study suggests that a perennial increase in an atmospheric nutrient deposition may compensate for the decrease in vertical nutrient supply due to stratification under the climate change scenario. Therefore, the ocean models must be coupled with the atmospheric models for a better forecast of a possible change in the ocean's primary production due to climate change.

Acknowledgements:

We would like to thank the Council of Scientific and Industrial Research (CSIR), Department of Science and Technology (DST), Satellite Application Centre (SAC), and Ministry of Earth Science (MoES) for funding in the collection and analysis of samples. The CSIR project CLICNIO (MLP1802) provides partial funding for this research. A.K. thanks the Department of Science and Technology, Govt. of India, for providing partial financial support under the Core research Grant (File no. CRG/2021/003307). We would like to thank Director for his encouragement and support. This has the NIO contribution number.....

Table 1: The collection period, area and publication details of the measured aerosols composition samples used in this study.

Cruise No.	Dates	Area	Reference
AS 430-528	11 April to 7 May 2006	Arabian Sea	14
SSK 60	24 Jan to 1 Feb 2014	Arabian Sea	Unpublished
SSK 77	11-20 Feb 2015	Arabian Sea	Unpublished
SS379	19-23 December 2018	Arabian Sea	19
AS602D-615D	19-17 December 2007	Arabian Sea	55
SSD29	20-30 November 2016	Arabian Sea	Unpublished
SS379	6-18 December 2018	Arabian Sea	19
AS417-864	31 March to 10 April 2006	Bay of Bengal	14
AS802-864	27 Dec 2008-28 January 2009	Bay of Bengal	16
SSK24	15-22 March 2017	Bay of Bengal	Unpublished
SSK118	24 March to 1 April 2018	Bay of Bengal	62
SN142	1-20 June 2019	Bay of Bengal	Unpublished
Coastal fixed station	September 2013 to December 2017	Bay of Bengal	25
AS 402-AS416	19-30 March 2006	Bay of Bengal	14
SSD40	5-31 August 2017	Arabian Sea	34
SSD55	2-30 August 2018	Arabian Sea	34
ST001	1-9 th June 2020	Bay of Bengal	Unpublished

Table 2: The slopes of long-term variability in AAOD, the concentration of mass, nitrate and ammonium in the aerosols at the selected regions in the northern Indian Ocean

Region	Region	Parameter	Winter	Spring	Summer	Fall	Annual
SWAS	53-58°E & 6-11°N	AAOD (/y)	0.003	0.004	-0.001 ^{\$}	0.005	0.002
		Mass ($\mu\text{g m}^{-3} \text{y}^{-1}$)	0.138	0.208	-0.062 ^{\$}	0.260	0.103
		NO ₃ ⁻ ($\mu\text{g m}^{-3} \text{y}^{-1}$)	0.004	0.006	-0.002 ^{\$}	0.009	0.003
		NH ₄ ⁺ ($\mu\text{g m}^{-3} \text{y}^{-1}$)	0.007	0.011	-0.003 ^{\$}	0.014	0.005
NWAS	58-61°E & 18-22°N	AAOD (/y)	0.002	0.002	-0.000*	0.006	0.002
		Mass ($\mu\text{g m}^{-3} \text{y}^{-1}$)	0.105	0.109	-0.009	0.338	0.109
		NO ₃ ⁻ ($\mu\text{g m}^{-3} \text{y}^{-1}$)	0.003	0.003	-0.0003	0.010	0.003
		NH ₄ ⁺ ($\mu\text{g m}^{-3} \text{y}^{-1}$)	0.006	0.006	-0.001	0.018	0.006
NEAS	66-69°E & 18-22°N	AAOD (/y)	0.007	0.002	-0.000*	0.012	0.004
		Mass ($\mu\text{g m}^{-3} \text{y}^{-1}$)	0.364	0.115	-0.014	0.659	0.221
		NO ₃ ⁻ ($\mu\text{g m}^{-3} \text{y}^{-1}$)	0.011	0.003	-0.0004	0.02	0.007
		NH ₄ ⁺ ($\mu\text{g m}^{-3} \text{y}^{-1}$)	0.019	0.006	-0.001	0.035	0.012
SEAS	73-76°E & 9-12°N	AAOD (/y)	0.013	0.013	0.0001*	0.012	0.008
		Mass ($\mu\text{g m}^{-3} \text{y}^{-1}$)	0.720	0.725	0.005*	0.685	0.443
		NO ₃ ⁻ ($\mu\text{g m}^{-3} \text{y}^{-1}$)	0.022	0.022	0.0002*	0.021	0.013
		NH ₄ ⁺ ($\mu\text{g m}^{-3} \text{y}^{-1}$)	0.038	0.038	0.0003*	0.036	0.023
NBoB	87-91°E & 17-21°N	AAOD (/y)	0.014	0.013	0.005	0.011	0.010
		Mass ($\mu\text{g m}^{-3} \text{y}^{-1}$)	1.667	1.523	0.593	1.33	1.176
		NO ₃ ⁻ ($\mu\text{g m}^{-3} \text{y}^{-1}$)	0.049	0.045	0.018	0.039	0.034
		NH ₄ ⁺ ($\mu\text{g m}^{-3} \text{y}^{-1}$)	0.110	0.098	0.039	0.081	0.076
SEBoB	90-94°E & 4-8°N	AAOD (/y)	-0.000*	0.001*	-0.000*	0.002*	0.000*
		Mass ($\mu\text{g m}^{-3} \text{y}^{-1}$)	-0.044	0.151	-0.053	0.246	0.049
		NO ₃ ⁻ ($\mu\text{g m}^{-3} \text{y}^{-1}$)	-0.001	0.004	-0.002	0.007	0.001
		NH ₄ ⁺ ($\mu\text{g m}^{-3} \text{y}^{-1}$)	-0.007*	0.012*	-0.001*	0.019 ^{\$}	0.005*
SWBoB	82-86°E & 4-8°N	AAOD (/y)	0.002 ^{\$}	0.002 ^{\$}	-0.001 ^{\$}	0.003 ^{\$}	0.001 ^{\$}
		Mass ($\mu\text{g m}^{-3} \text{y}^{-1}$)	0.199	0.222	-0.067	0.346	0.346 ^{\$}
		NO ₃ ⁻ ($\mu\text{g m}^{-3} \text{y}^{-1}$)	0.006	0.007	-0.002	0.010	0.010 ^{\$}
		NH ₄ ⁺ ($\mu\text{g m}^{-3} \text{y}^{-1}$)	0.011 ^{\$}	0.005*	0.002	0.031	0.013

^{\$} significant at p<0.05

* not significant

All others were significant at p<0.001

Table 3: The external source of nitrogen and its contribution to new production in the Arabian Sea and Bay of Bengal

External Source	Arabian Sea			Bay of Bengal			Reference
	TgN/y	%	NP TgC/y	TgN/y	%	NP TgC/y	
N ₂ fixation	4.4±4	70	29.0±26	0.2±0.1	7	1.3±0.7	55, 69, 70, 73-76
Rivers	0.1±0.03	2	0.7±0.2	1.7±0.4	60	11.2±3	67
SGD	0.06±0.03	1	0.4±0.2	0.1±0.02	3	0.7±0.1	51
Atm Dep	1.7±0.4	27	11.2±3	0.9±0.2	30	6.0±1	This study
Total	6.3±4		41.3±26	2.0±0.4		19.5±3	

% is percentage contribution to total sources

SGD is Submarine Groundwater Discharge

NP is new production computed based on a C/N ratio of 6.6.

References

1. R. A. Duce, P. S. Liss, J. T. Merrill, E. L. Atlas, P. Buat-Menard and B. Hicks et al., The atmospheric input of trace species to the world ocean, *Glob. Biogeochem. Cycles.*, 1991, 5, 193–259. <https://doi.org/10.1029/91GB01778>.
2. J. M. Prospero, The atmospheric transport of particles to the ocean, in *Particle Flux in the Ocean*, edited by V. Ittekkott, S. Honjo, and P. J. Depetris, SCOPE Rep. 1996, 57, 19– 52, John Wiley, New York, 1996.
3. T. Jickells and C. M. Moore, The importance of atmospheric deposition for ocean productivity. *Ann. Rev. Eco. Evol. and Sys.*, 2015, 46, 481-501.
4. N. M. Mahowald, Rachel Scanza, Janice Brahney, L. Christine, Goodale, G. Peter, Hess, J. Keith Moore and Jason Neff, Aerosol Deposition Impacts on Land and Ocean Carbon Cycles, *Current Climate Change Reports: 2017*, 3, 16-31.
5. R. A. Duce, J. ., K. Altieri, K. R. Arrigo, A. R. Baker, D. G. Capone, S. Cornell, F. Dentener, J. Galloway and R. S. Ganeshram et al., Impacts of atmospheric anthropogenic nitrogen on the open ocean, *Science.*, 2008, 320, 893–897.
6. N. Mahowald, K. Lindsay, D. Rothenberg, S. C. Doney, J. K. Moore, P. Thornton, J. T. Randerson and C. D. Jones, Desert dust and anthropogenic aerosol interactions in the Community Climate System Model coupled-carbon-climate model, *Biogeosci.*, 2011, 8, 387–414, doi: 10.5194/bg-8-387-2011.
7. P. W. Boyd, D. S. Mackie and K. A. Hunter, Aerosol iron deposition to the surface ocean: Modes of iron supply and biological responses, *Mar. Chem.*, 2010, 120, 128–143, doi:10.1016/j.marchem.2009.01.00.
8. C. Guieu, M. Al Azhar, O. Aumont, N. Mahowald, M. Levy, C. Ethé and Z. Lachkar, Major impact of dust deposition on the productivity of the Arabian Sea, *Geophy. Res. Lett.*, 2019, 46, 6736–6744. <https://doi.org/10.1029/2019GL082770>.
9. K. E Altieri, S. E Fawcett and M. G Hastings, Reactive nitrogen cycling in the atmosphere and ocean, *Ann. Rev. Ear. Planet. Sci.*, 2021, 49, 523-550.
10. S. C. Doney, N. Mahowald, I. Lima, R. A. Feely, F. T. Mackenzie, J. F. Lamarque and P. J. Rasch, Impact of anthropogenic atmospheric nitrogen and sulfur deposition on ocean acidification and the inorganic carbon system, *Proc. Natl. Acad. Sci.*, 2007, 104, 14580-14585. <https://doi.org/10.1073/pnas.0702218104>.
11. G. S. Okin, A. R. Baker, I. Tegen, N. M. Mahowald, F. J. Dentener, R. A. Duce, J. N. Galloway, K. Hunter, M. Kanakidou, N. Kubilay and J. M. Prospero, Impacts of atmospheric nutrient deposition on marine productivity: Roles of nitrogen, phosphorus and iron. *Glob. Biogeochem. Cycles.*, 2011, 25, <https://doi.org/10.1029/2010GB003858>.
12. T. D. Jickells, Nutrient biogeochemistry of the coastal zone, *Science.*, 1998, 284, 217 – 222.
13. J. Lelieveld, P. J. Crutzen, V. Ramanathan, M. O. Andreae, C. M. Brenninkmeijer, T. Campos and G. R. Cass, et. al., The Indian Ocean Experiment: Widespread air-pollution from South and Southeast Asia, *Science.*, 2001, 291, 1031-1036.

14. A. Kumar, A. Sudheer, and M. Sarin, Chemical characteristics of aerosols in MABL of Bay of Bengal and Arabian Sea during spring inter-monsoon a comparative study, *J. Earth Syst. Sci.*, 2008, 117, 325-332. <https://doi:10.1007/s12040-008-0035-9>.
15. K. K. Moorthy, S. N. Beegum, S. S. Babu, A. Smirnov, S. Rachel John, K. R. Kumar, K. Narasimhulu, C. Dutt and V. S. Nair, Optical and physical characteristics of Bay of Bengal aerosols during W-ICARB: spatial and vertical heterogeneities in the marine atmospheric boundary layer and in the vertical column, *J. Geophys. Res.*, 2010, 115, D24213, doi:10.1029/2010JD014094, 2010.
16. A. Kumar, A. K. Sudheer, V. Goswami and R. Bhushan, Influence of continental outflow on aerosol chemical characteristics over the Arabian Sea during winter, *Atmos. Environ.*, 2012, 50, 182–191.
17. P. R. Nair, K. George Susan, S. Aryasreea and Salu Jacob, Chemical composition of aerosols over Bay of Bengal during pre-monsoon: Dominance of anthropogenic sources, *J. Atm. and Solar-Terres. Phy.*, 2014, 109, 54-65. <http://dx.doi.org/10.1016/j.jastp.2014.01.004>.
18. A. R. Ashwini, P. Hegde, S. Aryasree, I. A. Girach and P. R. Nair, The continental outflow of anthropogenic aerosols over Arabian Sea and Indian Ocean during wintertime: ICARB-2018 campaign. *Sci. Total Environ.*, 2020, 712, 135214. <https://doi:10.1016/j.scitotenv.2019.135214>.
19. P. Bikkina, V. V. S. S. Sarma, Kimitaka Kawamura, B. Srinivas, K. Bhagawati and C. K. Sherin, Chemical characterization of wintertime aerosols over the Arabian Sea: Impact of marine sources and long-range transport, *Atm. Environ.*, 2020, 239, 117749.
20. J. Zhang and J. S. Reid, A decadal regional and global trend analysis of the aerosol optical depth using a data assimilation grade over-water MODIS and level 2 MISR aerosol products, *Atmos. Chem. Phys.*, 2010, 10, 10949–10963.
21. K. Yadav, V. D. Rao, B. Sridevi and V. V. S. S. Sarma, Decadal variations in natural and anthropogenic aerosols optical depth over the Bay of Bengal: Influence of pollutants from Indo-Gangetic Plain, *Environ. Pollu. Science Res.*, 2021, 28, 55202-55219. <https://doi:10.1007/s11356-021-14703-x>.
22. F. Schott and J. P. Mc Creary, The monsoon circulation of the Indian Ocean, *Prog. Oceanogr.*, 2001, 51, 1-123.
23. B. Srinivas, M. M. Sarin and V. V. S. S. Sarma, Atmospheric dry deposition of inorganic and organic nitrogen to the Bay of Bengal: Impact of continental outflow, *Mar. Chem.*, 2011, 127, 170-179. <https://doi:10.1016/j.marchem.2011.09.002>.
24. B. Srinivas, August Andersson, Elena N. Kirillova, Henry Holmstrand, Suresh Tiwari, A. K. Srivastava, D. S. Bisht and Örjan Gustafsson, Air quality in megacity Delhi affected by countryside biomass burning, *Nature Suatain.*, 2019, 2(3) <https://www.nature.com/articles/s41893-019-0219-0>.
25. V. R. Kumari, K. Yadav, V. V. S. S. Sarma and M. D. Kumar, Acidification of the coastal Bay of Bengal by aerosol deposition, *J. Earth Sys. Sci.*, 2021, 130, 223. <https://doi:10.1007/s12040-021-01723-x>.

26. P. K. Patra, M. D. Kumar, N. Mahowald and V. V. S. S. Sarma, Atmospheric deposition and surface stratification as controls of contrasting chlorophyll abundance in the North Indian Ocean, *J. Geophys. Res. Oceans.*, 2007, 112, C05029. doi:10.1029/2006JC003885.
27. P. Banerjee, and S. Prasanna Kumar, Dust-induced episodic phytoplankton blooms in the Arabian Sea during winter monsoon, *J. Geophys. Res.: Oceans.*, 2014, 119, 7123–7138. doi:10.1002/2014jc010304.
28. Z. Lachkar, Michael Mehari, Muchamad Al Azhar, Marina Lévy and Shafer Smith, Fast local warming is the main driver of recent deoxygenation in the northern Arabian Sea, *Biogeosci.*, 2021, 18, 5831–5849, 2021 <https://doi.org/10.5194/bg-18-5831-2021>.
29. M. M. Sarin, R. Rengarajan and S. Krishnaswami, Aerosol NO₃ and 210Pb distribution over the central-eastern Arabian Sea and their air-sea deposition fluxes, *Tellus B: Chemical and Physical Meteorology.*, 1999, 51(4): 749-758.
30. J. Lelieveld, P. J. Crutzen, V. Ramanathan, M. O. Andreae, C. A. M. Brenninkmeijer, and co-authors, The Indian Ocean experiment: widespread air pollution from South and Southeast Asia. *Science.*, 2001, 291, 1031-1036.
31. B. Srinivas and M. M. Sarin, Atmospheric dry-deposition of mineral dust and anthropogenic trace metals to the Bay of Bengal, *J. Mar. Sys.*, 2013, 126, 56-68. <http://dx.doi.org/10.1016/j.jmarsys.2012.11.004>.
32. K. Yadav, V. V. S. S. Sarma, D. B. Rao and M. D. Kumar, Influence of atmospheric dry deposition of inorganic nutrients on phytoplankton biomass in the coastal Bay of Bengal, *Mar. Chem.*, 2016, 187, 25-34. <https://doi.org/10.1016/j.marchem.2016.10.004>.
33. V. V. S. S. Sarma, M. S. Krishna, T. N. R. Srinivas, V. R. Kumari, K. Yadav and M. D. Kumar, Elevated acidification rates due to deposition of atmospheric pollutants in the coastal Bay of Bengal, *Geophys. Res. Lett.*, 2021, 48(16) <https://doi.org/10.1029/2021GL095159>.
34. M.A. Aswini, S. Tiwari, U. Singh, Siby Kurian, A. Patel, Sachin S. Gunthe and A. Kumar, Aeolian Dust and Sea Salt in Marine Aerosols over the Arabian Sea during the Southwest Monsoon: Sources and Spatial Variability, *ACS Earth and Space Chemistry* 2022 6 (4), 1044-1058, DOI: 10.1021/acsearthspacechem.1c00400
35. L. A. Bristow, C. M. Callbeck, M. Larsen, M. A. Altabet, J. Dekaezemacker, M. Forth, M. Gauns, R. N. Glud, M. M. Kuypers, G. Lavik, J. Milucka, S.W. A. Naqui, A. Pratihary, N. P. Revsbech, B. Thamdrup, A. H. Treusch and D. E. Canfield, N₂ production rates limited by nitrite availability in the Bay of Bengal oxygen minimum zone, *Nat. Geosci.*, 2017, 10, 24-29.
36. M. K. Roxy, K. Ritika, P. Terray, R. Murtugudde, K. Ashok and B. N. Goswami, Drying of Indian subcontinent by rapid Indian Ocean warming and a weakening land-sea thermal gradient, *Nat. Commun.*, 2015, 6(May), 7423, doi:10.1038/ncomms8423, 2015.
37. M. K. Roxy, Aditi Modi, M. Raghu Murtugudde, Vinu Valsala1, Swapna Panickal, S. Prasanna Kumar, M. Ravichandran, Marcello Vichi, and Marina Lévy, A reduction in marine primary productivity driven by rapid warming over the tropical Indian Ocean, *Geophys. Res. Lett.*, 2016, 43, 826-833. <http://dx.doi.org/10.1002/2015GL066979>.

38. J. Kurokawa, and T. Ohara, Long-term historical trends in air pollutant emissions in Asia: Regional Emission inventory in Asia (REAS) version 3, *Atmos. Chem. Phys.*, 2020, 20, 12761–12793. <https://doi.org/10.5194/acp-20-12761-2020>.
39. R. C. Levy, S. Mattoo, L. A. Munchak, L. A. Remer, A. M. Sayer, F. Patadia and N. C. Hsu, The Collection 6 MODIS aerosol products over land and ocean, *Atmospheric Measurement Techniques*, 2013, 6, 2989–3034, <https://doi.org/10.5194/amt-6-2989-2013>.
40. J. Wei, Z. Li, Y. Peng and L. Sun, MODIS Collection 6.1 aerosol optical depth products over land and ocean: validation and comparison, *Atmos. Environ.*, 2019, 201, 428–440, <https://doi.org/10.1016/j.atmosenv.2018.12.004>, 2019.
41. Y. J. Kaufman, O. Boucher, D. Tanré, M. Chin, L. A. Remer and T. Takemura, Aerosol anthropogenic component estimated from satellite data, *Geophys. Res. Lett.*, 2005, 32(17).
42. Y. J. Kaufman, A. Smirnov, B. N. Holben and O. Dubovik, Baseline maritime aerosol: Methodology to derive the optical thickness and scattering, properties, *Geophys. Res. Lett.*, 2001, 28, 3251–3254.
43. L. J. Spokes, S. G. Yeatman, S. E. Cornell and T. D. Jickells, Nitrogen deposition to the eastern Atlantic Ocean. The importance of south-easterly flow. *Tellus B.*, 2000, 52, 37-49.
44. Y. Chen, S. Mills, J. Street and D. Golan, A. Post, and co-authors, Estimates of atmospheric dry deposition and associated input of nutrients to Gulf of Aqaba seawater, *J. Geophys. Res.*, 2007, 112, D04309.
45. B. D. Santer, T. M. L. Wigley, J. S. Boyle, D. J. Gaffen, J. J. Hnilo, D. Nychka, D. E. Parker and K. E. Taylor, Statistical significance of trends and trend differences in layer-average atmospheric temperature time series. *J. Geophys. Res.*, 2000, 105, 7337–7356. <https://doi.org/10.1029/1999jd901105>.
46. F. Li and V. Ramanathan, Winter to summer monsoon variation of aerosol optical depth over the tropical Indian Ocean, *J. Geophys. Res.*, 2002, 107, 4284. <https://doi.org/10.1029/2001JD000949>.
47. M. M. Sarin, A. Kumar, B. Srinivas, A. K. Sudheer and N. Rastogi, Anthropogenic sulphate aerosols and large Cl-deficit in marine atmospheric boundary layer of tropical Bay of Bengal, *J. Atmos. Chem.*, 2010, 66, 1-10.
48. S. Kumar, N. Singh, R. P. Singh and Devendraa Singh, Variability of air quality and aerosol over Indian region during 2003-2012, *Indian J. Phys.*, 2022, doi.org/10.1007/s12648-022-02375-3.
49. P. P. Pease, V. P. Tchakerian, and N.W. Tindale, Aerosols over the Arabian Sea: geochemistry and source areas for aeolian desert dust, *J. Arid Environ.*, 1998, 39, 477–496.
50. J. F. Le´on, and M. Legrand, Mineral dust sources in the surroundings of the north Indian Ocean, *Geophys. Res. Lett.*, 2003, 30, 1309, [doi:10.1029/2002GL016690](https://doi.org/10.1029/2002GL016690), 2003.

51. B. S. K. Kumar, R. Viswanadham, V. R. Kumari, D. B. Rao, M. H.K. Prasad, N. Srinivas and V. V. S. S. Sarma, Spatial variations in dissolved inorganic nutrients in the groundwaters along the Indian coast and their export to adjacent coastal waters, *Environ. Sci. Pollut. Res.*, 2021, doi:10.1007/s11356-020-11387-7.
52. K. Suresh, A. Kumar, V. Ramaswamy and C. Prakash Babu, Seasonal variability in Aeolian dust deposition fluxes and their mineralogical composition over the Northeastern Arabian Sea, *Int. J. Environ. Sci. Technol.*, 2021, <https://doi.org/10.1007/s13762-021-03503-y>.
53. S. K. Satheesh and J. Srinivasan, Enhanced aerosol loading over Arabian Sea during the pre-monsoon season: Natural or anthropogenic?, *Geophys. Res. Lett.*, 2002, 29, 1874, doi:10.1029/2002gl015687.
54. J. Jose, B. Srimuruganandam and S. M. S. Nagendra, Characterization of PM10 and PM2.5 emission sources at Chennai, India, *Nat. Env. And Poll. Tech.*, 2019, 18, 555-562.
55. S. Kumar, R. Ramesh, R. M. Dwivedi, Mini Raman, M. S. Sheshshayee and W. D'Souza, Nitrogen uptake in the northeastern Arabian Sea during winter cooling, *Int. J. Oceanogr.*, 2010, 819029, doi:10.1155/2010/819029.
56. M.K. Soman and K.K. Kumar, Some Aspects of daily rainfall distribution over India during the South-West Monsoon Season, *Int. Jl. of Climat.*, 1990, 10(3), 299 – 311.
57. R. T. Barber, John Marra, Robert R. Bidigare, Louis A. Codispoti, David Halpern, Zackary Johnson, Mikel Latasa, Ralf Goericke and Sharon L. Smith, Primary productivity and its regulation in the Arabian Sea during 1995, *Deep-Sea Res., Part II*, 2001, 48, 1127–1172.
58. P. M. A. Bhattathiri, A. Pant, S. Sawant, M. Gauns, S. G. P. Matondkar and R. Mohanraju, Phytoplankton production and chlorophyll distribution in the eastern and central Arabian Sea in 1994—1995, *Curr. Sci.*, 1996, 71, 857–862.
59. M. Gauns, M. Madhupratap, N. Ramaiah, R. Jyothibabu, V. Fernandes, J. T. Paul and S. Prasanna Kumar, Comparative accounts of biological productivity characteristics and estimates of carbon fluxes in the Arabian Sea and Bay of Bengal, *Deep. Sea. Res., II*, 2005, 52, 2003–2017.
60. V. V. S. S. Sarma, H. B. Dalabehra, P. Sudharani, R. Remya, J. S. Patil and D. V. Desai, Variations in the inorganic carbon components in the thermal fronts during winter in the northeastern Arabian Sea, *Mar. Chem.*, 2015, 169, 16-22. <https://doi.org/10.1016/j.marchem.2014.12.009>.
61. V. V. S. S. Sarma, L. Jagadeesan, H. B. Dalabehra, D. N. Rao, G. S. Kumar, D. S. Durgadevi, K. Yadav, S. Behera and M. M. R. Priya, Role of eddies on intensity of oxygen minimum zone in the Bay of Bengal, *Cont. Shelf. Res.*, 2018, 168, 48–53. doi:10.1016/j.csr.2018.09.008.
62. V. V. S. S. Sarma, and H. B. Dalabehra. New and primary production in the western Indian Ocean during fall monsoon, *Mar. Chem.*, 2019, 215, 103687, doi:10.1016/j.marchem.2019.103687.
63. V. V. S. S. Sarma, D. N. Rao, G. R. Rajula, H. B. Dalabehra and K. Yadav, Organic nutrients support high primary production in the Bay of Bengal, *Geophys. Res. Lett.*, 2019, 46, 2019GL082262–. doi:10.1029/2019GL082262.

64. P. Bikkina, V. V. S. S. Sarma, Kimitaka Kawamura and B. Srinivas, Dry-deposition of inorganic and organic nitrogen aerosols to the Arabian Sea: Sources, transport and biogeochemical significance in surface waters, *Mar. Chem.*, 2021, 231, 103938. <https://doi.org/10.1016/j.marchem.2021.103938>.
65. V. V. S. S. Sarma and H. Dalbehara, New primary production in the western Indian Ocean during fall monsoon, *Mar. Chem.*, 2019, 215(45), 103687. DOI: 10.1016/j.marchem.2019.103687.
66. M. S. Krishna, V. R. Prasad, V. V. S. S. Sarma, N. P. C. Reddy, K. P. J. Hemalatha, and co-authors, Fluxes of dissolved organic carbon and nitrogen to the northern Indian Ocean from the Indian monsoonal rivers, *J. Geophys. Res. (Biogeosciences)*, 2015, 120, 2067–2080.
67. V. V. S. S. Sarma, M. S. Krishna, V.D. Rao, R. Viswanadham, N. A. Kumar and V. R. Kumari, et al., Sources and Sinks of CO₂ in the west coast of Bay of Bengal; *Tellus B.*, 2012, 64 10961, doi: 3402/tellusb.v64i0.10961.
68. D. G. Capone, A. Subramaniam, J. P. Montoya, M. Voss, C. Humborg, A. M. Johansen, R. L. Siefert and E. J. Carpenter, There is an extensive bloom of the N₂-fixing cyanobacterium *Trichodesmium erythraeum* in the central Arabian Sea, *Mar. Ecol. Prog. Ser.*, 1998, 172, 281–292, doi:10.3354/meps172281.
69. Gandhi Naveen, Aravind Singh, S. Prakash, R. Ramesh, Mini Raman, M. S. Sheshshayee and Shetye Suhas, First measurements of N₂ fixation during a *Trichodesmium* bloom in the eastern Arabian Sea, *Glob. Biogeochem. Cycles.*, 2011, 25, doi:10.1029/2010gb003970.
70. P. Bhavya, S. Kumar, G. Gupta, V. Sudheesh, K. Sudharma and D. Varrier, et al., Nitrogen uptake dynamics in a tropical eutrophic estuary (Cochin, India) and adjacent coastal waters. *Estuar. Coasts.*, 2016, 39, 54–67. doi: 10.1007/s12237-015-9982-y.
71. P. Kumar, A. Singh, R. Ramesh and T. Nallathambi, N₂ Fixation in the Eastern Arabian Sea: Probable Role of Heterotrophic Diazotrophs *Frontiers, Mar. Sci.*, 2017, 4, 80.
72. A. Ahmed, M. Gauns, S. Kurian, P. Bardhan, A. Pratihary and H. Naik, et al., Nitrogen fixation rates in the eastern Arabian Sea. *Estuar., Coastal and Shelf Sci.*, 2017, 191, 74–83. <https://doi.org/10.1016/j.ecss.2017.04.005>.
73. V. V. S. S. Sarma, R. Vivek, D. N. Rao and V. R. D. Ghosh, Severe phosphate limitation on nitrogen fixation in the Bay of Bengal, *Cont. Shelf. Res.*, 2020, 205, 104199.
74. Himanshu Saxena, Deepika Sahoo, Mohammad Atif Khan, Sanjeev Kumar, A. K. Sudheer and Arvind Singh, Dinitrogen fixation rates in the Bay of Bengal during summer monsoon, *Environ. Res. Commun.*, 2020, 2, 051007 doi:10.1088/2515-7620/ab89fa.
75. V. R. Kumari, V.V.S.S. Sarma and M. Dileep Kumar, Spatial variability in aerosol composition and its seawater acidification potential in coastal waters of the western coastal Bay of Bengal, *J. Earth Syst. Sci.*, 2022 (under review).
76. N. D. Rao, V. R. D. Ghosh, P. Sam, K. Yadav and V. V. S. S. Sarma, Phosphate removal through adsorption on suspended matter in the Bay of Bengal: Possible implications to primary production. *J. Earth Syst. Sci.*, 130 (2021), p. 22, 10.1007/s12040-020-01524-8.

77. R. C. Dugdale, and J. J. Goering, Uptake of new and regenerated forms of nitrogen in primary productivity, *Limnol. Oceanogr.*, 1967, 12, 196-206.
78. K. O. Buesseler, L. Ball, J. Andrews, C. Benitez-Nelson, R. Belostock, F. Chai and Y. Chao, Upper Ocean export of particulate organic carbon in the Arabian Sea derived from Thorium-234, *Deep-Sea Res. II*, 1998, 2461–2487.
79. S. S. Anand, R. Rengarajan, V. V. S. S. Sarma, A. K. Sudheer, R. Bhushan and S. K. Singh, Spatial variability of upper ocean POC export in the Bay of Bengal and the Indian Ocean determined using particle-reactive ^{234}Th , *J. Geophys. Res. Oceans.*, 2017, 122. <https://doi.org/10.1002/2016JC012639>.
80. S. S. Anand, R. Rengarajan and V. V. S. S. Sarma, ^{234}Th based carbon export flux along the Indian GEOTRACES GI02 section in the Arabian Sea and the Indian Ocean. *Glob. Biogeochem. Cycles.*, 2018, <https://doi.org/10.1002/2017GB005847>.
81. L. Dong, T. Zhou, and B. Wu, Indian Ocean warming during 1958–2004 simulated by a climate system model and its mechanism, *Clim. Dynam.*, 2014, 42, 203–217, doi.org/10.1007/s00382-013-1722-z (2014), 2014.
82. V. V. S. S. Sarma, M. S. Krishna, Y. S. Paul and V. S. N. Murthy, Observed changes in ocean acidity and carbon dioxide exchange in the coastal Bay of Bengal - a link to air pollution, *Tellus B*, 2015, 67, 24638. <https://doi.org/10.3402/tellusb.v67.24638>.
83. N. L. Bindoff, W. W. L. Cheung, J. G. Kairo, J. Arístegui, V. A. Guinder and R. Hallberg, et al., Changing Ocean, Marine Ecosystems, and Dependent Communities. 2019, IPCC Special Report on the Ocean and Cryosphere in a Changing Climate.

Legend to figures

Write NEAS, SEAS, NWAS, SWAS, NBoB, SWBoB and SEBoB to be given

Figure 1: Monthly variations in anthropogenic AOD (AAOD) in the northern Indian Ocean

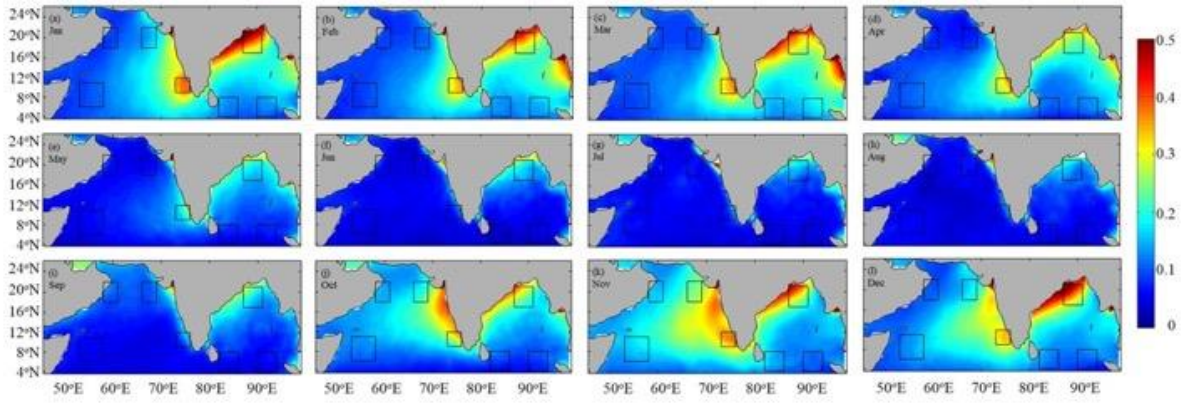


Figure 2: Distribution of measured a) mass, b) nitrate and c) ammonium concentrations during different periods in the northern Indian Ocean

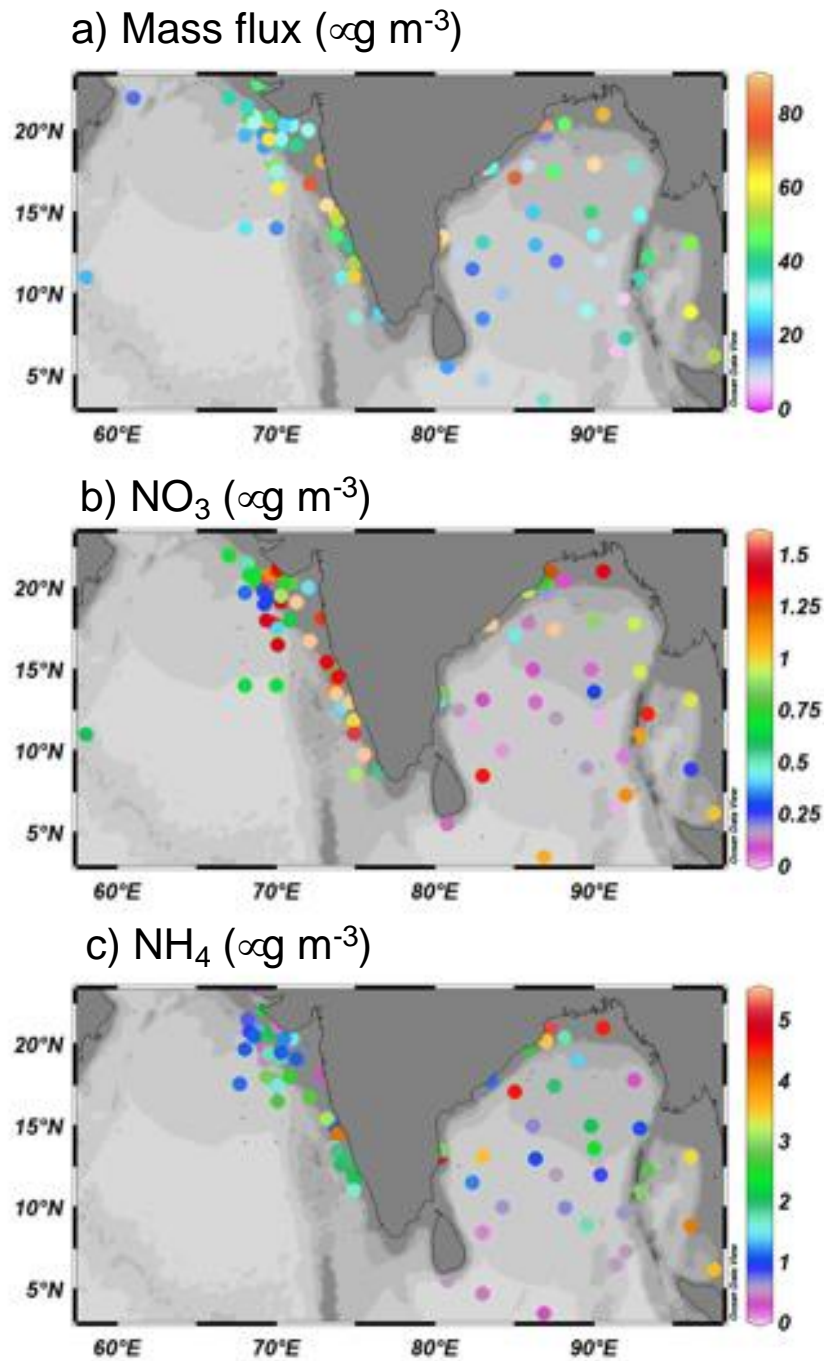


Figure 3: Linear relationship of AAOD with a) mass, b) Nitrate and c) ammonium in the aerosols over the Arabian Sea (red) and Bay of Bengal (blue).

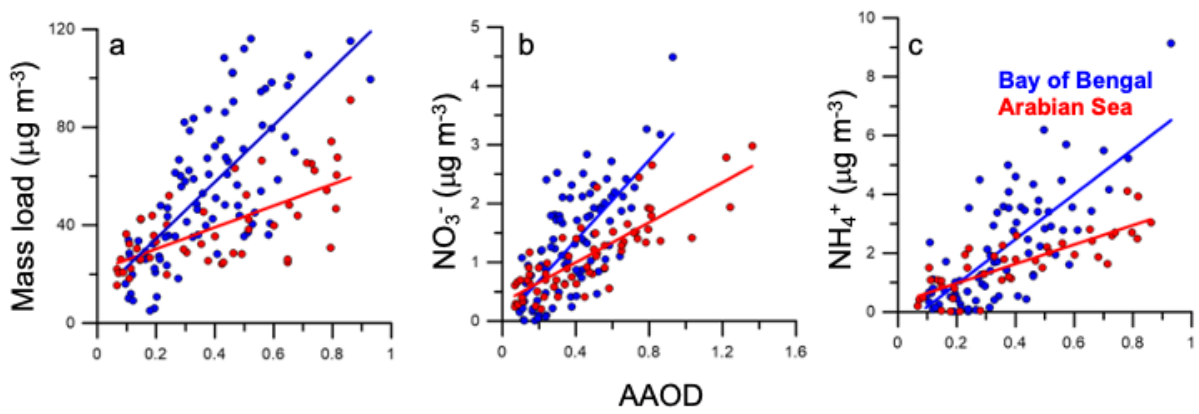


Figure 4: The estimated climatological monthly mean (2001-2020) mass of aerosols in the northern Indian Ocean

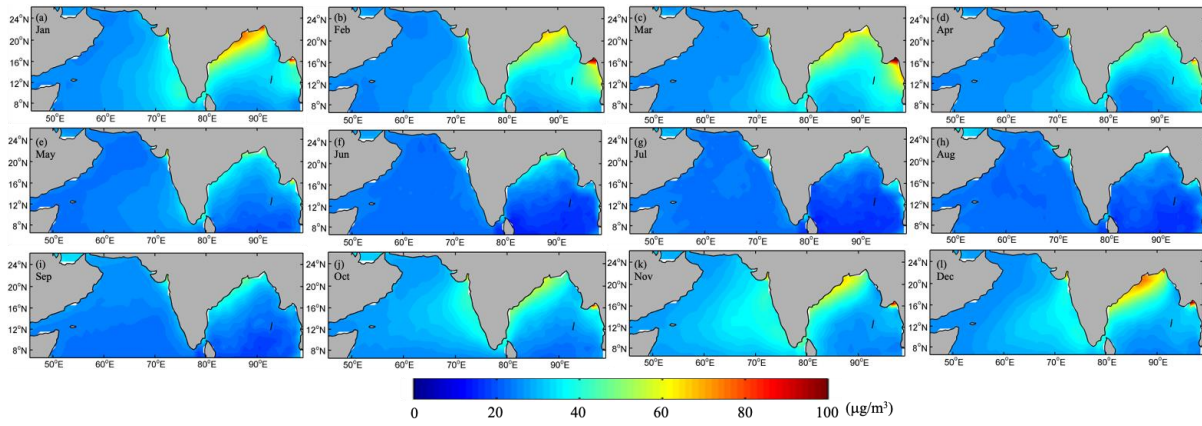


Figure 5: The estimated climatological monthly mean (2001-2020) nitrate concentrations in the aerosols in the northern Indian Ocean

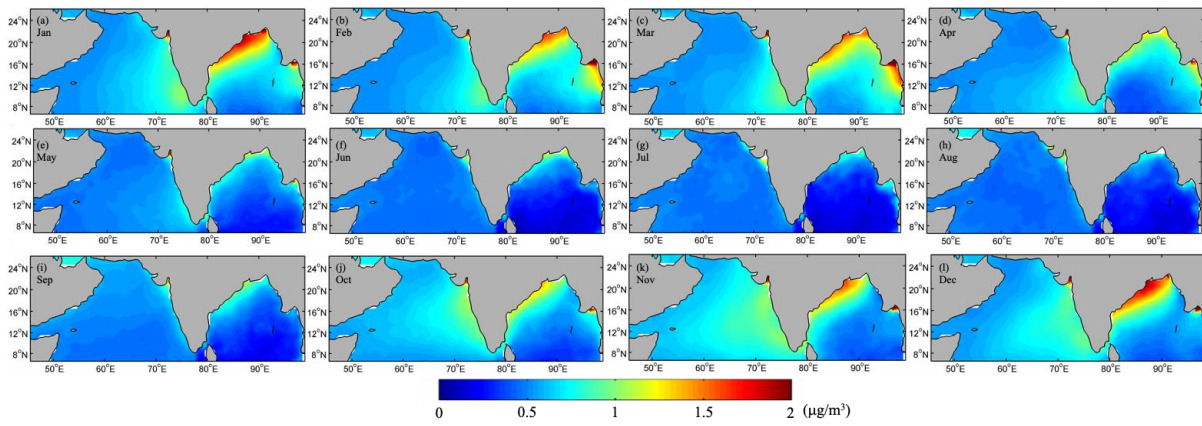


Figure 6: The estimated climatological monthly mean (2001-2020) ammonium concentrations in the aerosols in the northern Indian Ocean

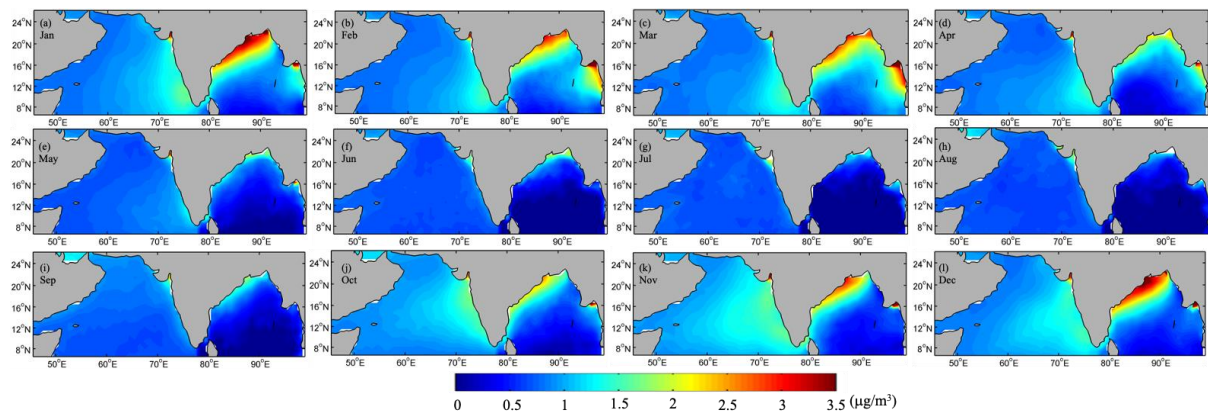


Figure 7: The estimated climatological monthly mean (2001-2020) nitrate depositional flux in the northern Indian Ocean

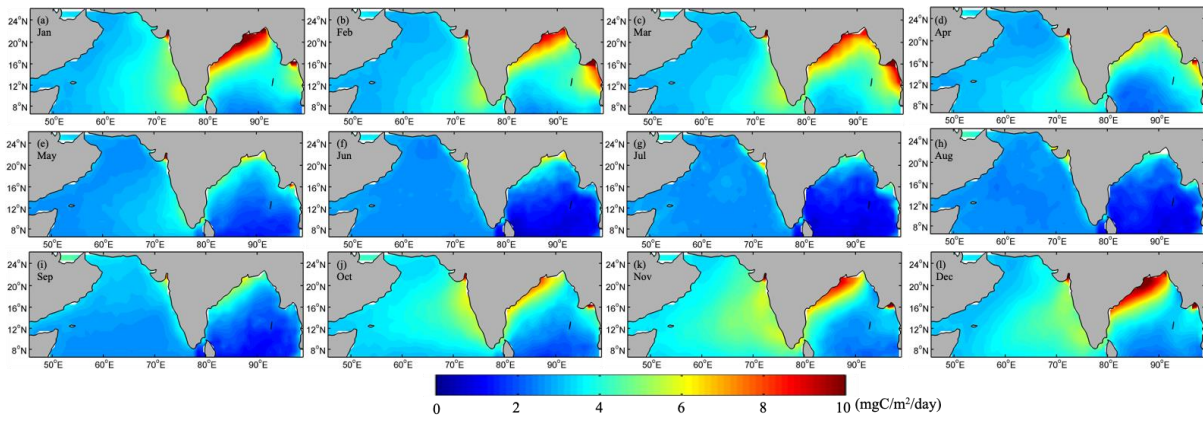


Figure 8: The estimated climatological monthly mean (2001-2020) ammonium depositional flux in the northern Indian Ocean.

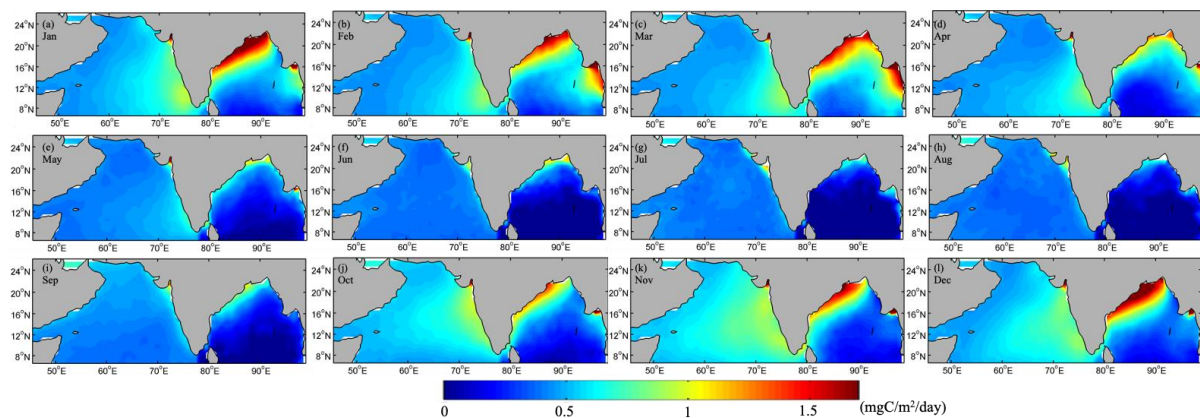


Figure 9: a) Measured primary production integrated to the upper 5 m in the northern Indian Ocean, b) estimated primary production due to deposition of nitrate, c) estimated primary production due to deposition of ammonium and d) the contribution of primary production due to deposition of nitrate and ammonium to total primary production in the upper 5 m of the water column.

